

# Newly Developed Dual Topoisomerase Inhibitor P8-D6 is Highly Active in Ovarian Cancer

**Inken Flörkemeier**

University Medical Centre Schleswig-Holstein <https://orcid.org/0000-0001-5885-6352>

**Tamara N. Steinhauer**

Christian-Albrechts-University Kiel, Pharmaceutical Institute

**Nina Hedemann**

University Medical Centre Schleswig-Holstein

**Magnus Ölander**

Uppsala University

**Per Artursson**

Uppsala University

**Bernd Clement**

Christian-Albrechts-University Kiel, Pharmaceutical Institute

**Dirk O. Bauerschlag** (✉ [Dirk.bauerschlag@uksh.de](mailto:Dirk.bauerschlag@uksh.de))

University Medical Centre Schleswig-Holstein

---

## Research

**Keywords:** OvCa, chemotherapy, drug development, dual topoisomerase inhibitor, apoptosis, 2D, 3D, co-culture, primary cells, hepatotoxicity

**Posted Date:** July 28th, 2021

**DOI:** <https://doi.org/10.21203/rs.3.rs-743550/v1>

**License:**  This work is licensed under a Creative Commons Attribution 4.0 International License.

[Read Full License](#)

---

**Version of Record:** A version of this preprint was published at Therapeutic Advances in Medical Oncology on January 1st, 2021. See the published version at <https://doi.org/10.1177/17588359211059896>.



RESEARCH

1 **Newly developed dual topoisomerase inhibitor P8-**  
2 **D6 is highly active in ovarian cancer**

3 **Inken Flörkemeier<sup>1,2</sup>, Tamara N. Steinhauer<sup>2</sup>, Nina Hedemann<sup>1</sup>, Magnus Ölander<sup>3</sup>, Per**  
4 **Artursson<sup>3</sup>, Bernd Clement<sup>2</sup> and Dirk O. Bauerschlag<sup>1,\*</sup>**

5 <sup>1</sup> University Medical Centre Schleswig-Holstein, Campus Kiel, Department of Gynaecology and Obstetrics,  
6 Kiel, Germany

7 <sup>2</sup> Christian-Albrechts-University Kiel, Pharmaceutical Institute, Department of Pharmaceutical and  
8 Medicinal Chemistry, Kiel, Germany

9 <sup>3</sup> Uppsala University, Department of Pharmacy, Uppsala, Sweden

10 \* Correspondence: Dirk Bauerschlag ([dirk.bauerschlag@uksh.de](mailto:dirk.bauerschlag@uksh.de)), University Medical Centre Schleswig-  
11 Holstein, Campus Kiel, Department of Gynaecology and Obstetrics, Arnold-Heller-Str. 3; 24105 Kiel

12

## 13 **Abstract:**

### 14 **Background**

15 Ovarian cancer (OvCa) constitutes a rare and highly aggressive malignancy and is one of the most  
16 lethal of all gynaecologic neoplasms. Due to chemotherapy resistance and treatment limitations  
17 because of side effects, OvCa is still not sufficiently treatable. Hence, new drugs for OvCa therapy  
18 such as P8-D6 with promising antitumour properties have a high clinical need. The  
19 benzo[c]phenanthridine P8-D6 is an effective inducer of apoptosis by acting as a dual  
20 topoisomerase I/II inhibitor.

### 21 **Methods**

22 In the present study, the effectiveness of P8-D6 on OvCa was investigated *in vitro*. In various  
23 OvCa cell lines and *ex vivo* primary cells, the apoptosis induction compared to standard  
24 therapeutic agents was determined in 2D monolayers. Expanded by 3D and co-culture, the P8-D6  
25 treated cells were examined for changes in cytotoxicity, apoptosis rate and membrane integrity via  
26 scanning electron microscopy (SEM). Likewise, the effects of P8-D6 on non-cancer human ovarian  
27 surface epithelial cells and primary human hepatocytes were determined.

### 28 **Results**

29 This study shows a significant P8-D6-induced increase in apoptosis and cytotoxicity in OvCa cells  
30 which surpasses the efficacy of standard therapeutic drugs. Non-cancer cells were affected only  
31 slightly by P8-D6. Moreover, no hepatotoxic effect in *in vitro* studies was detected.

### 32 **Conclusions**

33 P8-D6 is a strong and rapid inducer of apoptosis and might be a novel treatment option for OvCa  
34 therapy.

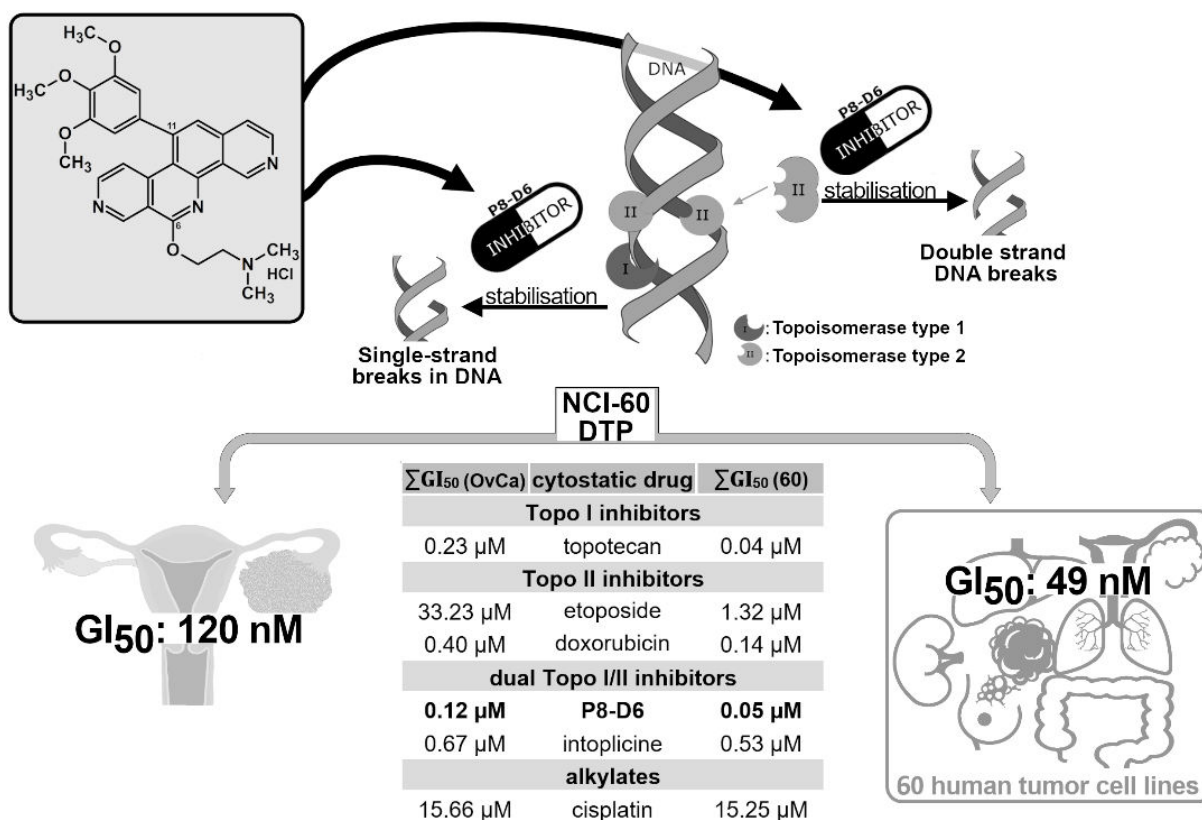
35

36 **Keywords:** OvCa, chemotherapy; drug development; dual topoisomerase inhibitor; apoptosis, 2D,  
37 3D, co-culture, primary cells, hepatotoxicity,

## 38 **Background**

39 Ovarian cancer (OvCa) is the fifth leading cause of cancer deaths among women and the most  
40 lethal gynaecological malignancy in the developed world (1). The frequent diagnosis in advanced  
41 stages and insufficient treatment options due to chemotherapy resistance and side effects lead to a  
42 poor prognosis. First line therapy usually consists of surgical cytoreduction followed by  
43 platinum/taxane-based combination chemotherapy, but most patients relapse with drug-resistance  
44 in the course of the disease (2). Previous studies demonstrated a benefit in second line therapy with  
45 topoisomerase inhibitors like liposomal doxorubicin or topotecan. However, response duration was  
46 commonly short (3). Consequently, an important aim is to reduce mortality by improved new  
47 therapeutic options.

48 P8-D6 acts as a dual topoisomerase poison by stabilizing the covalent Topo-DNA-intermediate  
49 of both topoisomerase (Topo) enzymes I and II (4). Topoisomerases regulate torsional stress in  
50 DNA to enable essential genome functions (e.g. transcription, replication, or recombination). Topo I  
51 causes single strand breaks while Topo II with its isoforms  $\alpha$  and  $\beta$  is responsible for the double-  
52 strand break (5, 6) (Fig. 1). Such topoisomerase poisoning leads to cell death by inducing apoptosis.  
53 The aza-analogous Benzo[*c*]phenanthridine P8-D6 was synthesized in an optimized four-step  
54 process with advantageous physicochemical and cytotoxic properties (7). In the NCI-60 DTP  
55 Human Tumor Cell Line screening 49 nM of P8-D6 results in an average growth inhibition of 50 %  
56 ( $GI_{50}$ ) (7, 8). The result for OvCa cell lines were 0.12  $\mu$ M compared to cisplatin with 15.25  $\mu$ M or  
57 topotecan with 0.23  $\mu$ M, respectively.



58

59 **Fig. 1. Chemical structure and mechanism of P8-D6 action.** P8-D6 acts as a dual topoisomerase inhibitor  
 60 by stabilising the cleavable Topo–DNA complex, thereby inducing apoptosis. The effectiveness and the  
 61 broad activity spectrum of P8-D6 were examined for the first time in a 60-tumour cell line panel by the  
 62 NCI. In the evaluation, P8-D6 reached an average  $\Sigma GI_{50}$  (60) value of 49 nM in multiple tumour cell lines  
 63 (7). For the ovarian carcinoma cells tested, this  $GI_{50}$  average was 0.12  $\mu$ M. For comparison, other active  
 64 drugs are listed.  $\Sigma GI_{50}$  (60): average growth inhibition 50% in 60 cancer cell lines (different cancer types),  
 65  $\Sigma GI_{50}$  (OvCa): average growth inhibition 50% in OvCa cell lines.

66 Cell-based assays are an important pillar in drug development. In addition to traditional two-  
 67 dimensional (2D) monolayer, co-culture and three-dimensional (3D) cell culture have recently  
 68 gained importance because of greater comparability with *in vivo* set ups (9). Therefore, efficacy  
 69 studies of P8-D6 were performed on different OvCa cell lines and patient derived primary cells,  
 70 compared to single drugs and combinational drug therapy. (10–12).

71 Preclinical cancer drug development addressed several topics, including target achievement,  
 72 induction of apoptosis in cancer cells and toxicity in normal cells.

## 73 **Methods**

### 74 **Materials**

75 P8-D6 was synthesized as recently described (7) and solved in PBS. Topotecan, etoposide,  
76 cisplatin and doxorubicin were obtained from the UKSH dispensary.

### 77 **In vitro experiments**

78 **Cell Preparation and Culture:** Human OvCa cell lines A2780, HEY, Igrov-1, OvCar8, SKOV-3 and  
79 fibroblasts Detroit 551 were maintained in RPMI 1640 supplemented with 10 % FBS, 60 IU( $\mu$ g)/ml  
80 penicillin–streptomycin. SKOV-3luc (firefly luciferase gene) were grow in DMEM, supplemented  
81 with 10 % FBS, 800  $\mu$ g/ml neomycin. Primary OvCa cells were isolated from advanced stage OvCa  
82 patients during surgery at first diagnosis (UKSH, Campus Kiel). The tumour cells were extracted  
83 from tumour tissue and ascites as described previously (13, 14). Human ovarian surface epithelial  
84 cells (HOSE) (Innoport) were cultivated in OSE medium containing 1% OEpiCGS, 100 IU( $\mu$ g)/ml  
85 penicillin–streptomycin. Primary human hepatocytes were isolated from liver tissue under surgery  
86 (Uppsala University Hospital), isolated and cultured as described previously (15). Cells were grown  
87 at 37°C, 5 % CO<sub>2</sub> and short tandem repeat profiling (16) and mycoplasma contamination by  
88 MycoAlert™ (Lonza) were checked.

89 Informed consent was obtained from all donors, in agreement with the approval from the  
90 Institutional Review Board of the UKSH, Campus Kiel (AZ: D578/20) and the Uppsala Regional  
91 Ethical Review Board (Ethical Approval 2009/028).

92 **Western Blot:** Cells were harvested, protein contents determined and SDS-PAGE and Western Blot  
93 analysis was carried out as described previously (17). Membranes were incubated with primary  
94 antibodies (anti-TopoI 1:500 (Santa Cruz#sc-271285), anti-TopoII $\alpha$ / $\beta$  1:10000 (Abcam#ab109524),  
95 anti-HSP 90 1:10000 (Santa Cruz#sc-13119)) and HRP-labelled anti-mouse IgG 1:2000 (Santa  
96 Cruz#sc-516102) or HRP-labelled goat anti-rabbit IgG 1:3000 (Elabscience#E-AB-1003)

97 Chemiluminescence was visualized using ECL Plus Western Blotting Detection System and  
98 ChemoStar ECL & Fluorescence Imager (Intas).

99 **Fluorescence Imaging:** Due to its chemical structure, P8-D6 has fluorescent properties (462<sub>Ex</sub>/530<sub>Em</sub>).  
100 10000 cells/well were seeded in glass-bottomed 4-well chamber slides and treated with 10  $\mu$ M P8-  
101 D6 or PBS for 30 min, washed with PBS and fixed with acetone (10 min at RT). Samples were  
102 stained by CellTracker™ Deep Red Dye (5  $\mu$ M at 37 °C for 15 min) and DAPI (0.5  $\mu$ g/ml)  
103 (Vectashield). Fluorescence imaging was performed using DAPI (350<sub>Ex</sub>/470<sub>Em</sub>), FITC (490<sub>Ex</sub>/525<sub>Em</sub>)  
104 and Cy5 (649<sub>Ex</sub>/670<sub>Em</sub>) filters. Microscope Axioplan 2 (Carl Zeiss Microscopy), Isis Version 5.8.8.  
105 (MetaSystems).

106 **2D Viability & Apoptosis Assay:** 10,000 cells/well were seeded in a 96-well plate (Corning #3903)  
107 and treated for 48 h. The measurement using ApoLive-Glo™ Multiplex Assay (Promega #G6410)  
108 was performed as described in the instruction (TM325) with a microplate reader (Infinite 200,  
109 Tecan). Relative caspase activity: caspase activity divided by the viability (normalized to control).  
110 With viability data dose-response curves were plotted and IC<sub>50</sub> values were calculated (GraphPad).

111 **Flow Cytometric Analysis:** Cells were seeded in 6-well plates and treated for 48 h. Cells were  
112 harvested and stained as described previously (17).

113 **3D Cytotoxicity, Viability & Apoptosis Assay:** A2780 (200/well), SKOV-3 (8000/well), OvCar8  
114 (1000/well) and HEY (450/well) cells were seeded into a 96-well ULA plate (Corning #4520) and  
115 grown for 96 h. Then, spheroids were treated for 48 h. Simultaneously, CellTox™ Green assay  
116 (Promega #G8731) was added and detected (485<sub>Ex</sub>/520<sub>Em</sub>) 24 h and 48 h after treatment using  
117 NYONE® (SYNENTEC). Filters: BF<sub>Ex</sub>/Green<sub>Em</sub>(530/43 nm); Blue<sub>Ex</sub>(475/28 nm)/Green<sub>Em</sub>(530/43 nm).  
118 Subsequently, viability and apoptosis were determined by RealTime-Glo™ (460<sub>Em</sub>) (Promega  
119 #G9711) and Caspase-Glo 3/7 (565<sub>Em</sub>) (Promega # G8090) using microplate reader (Infinite 200,  
120 Tecan). The measurement was performed according to the instructions. Relative caspase activity:  
121 caspase activity divided by the viability (normalized to control)). For live-dead staining, cells were

122 grown and treated as described above. Then, 80 % of the medium was removed and replaced with  
123 propidium iodide (PI) (10 µg/ml), calcein-AM (1 mM) and hoechst 33342 (0.001 %) in medium for  
124 3 h and imaged by NYONE® (SYNENTEC). Filters: BF<sub>Ex</sub>/Green<sub>Em</sub>(530/43nm); hoechst33342:  
125 UV<sub>Ex</sub>(377/50nm)/Blue<sub>Em</sub>(452/45nm); calcein-AM: Blue<sub>Ex</sub>(475/28nm)/Green<sub>Em</sub> (530/43nm); PI:  
126 Lime<sub>Ex</sub>(562/40nm)/Red<sub>Em</sub>(628/32nm).

127 **Scanning Electron Microscopy (SEM):** Spheroids were grown as described above, treated with  
128 1 µM P8-D6 and PBS for 48 h and fixed with 2.5% glutaraldehyde (1 h RT) and then 1% osmium  
129 tetroxide (1.5 h RT). Spheroids were dehydrated with ethanol [25, 50, 75, 96, 100 %] and air dried  
130 using hexamethyldisilazane on charcoal stubs overnight. Then, spheroids were coated with gold  
131 and measured with SEM (Phenom XL).

132 **Co-culture:** For co-culture, 40,000 Detroit 551 fibroblasts were seeded into 24-well plates and 40,000  
133 A2780 were cultured onto inserts (ThinCert™ translucent 0.4µm). Cells were treated for 48 h. Cells  
134 were harvested and centrifuged (10 min, 250 g). Cell pellets were resuspended in 25 µl medium.  
135 Viability and apoptosis were measured using ApoLive-Glo™ Multiplex Assay.

136 **Hepatotoxicity:** Oxidative stress of hepatocytes caused by 48 h treatment was analysed via  
137 dihydroethidium fluorescence. The cell culture protocol was previously described (15). Apoptosis  
138 was analysed using ApoLive-Glo™ Multiplex Assay.

139 **Statistical Analysis:** Statistical tests were performed using GraphPad Prism9 (GraphPad). Gaussian  
140 distribution was tested by Shapiro-Wilk normality test. Data of multiple groups were checked with  
141 one-way ANOVA for statistical significance. Statistically significant differences were assumed at *p*-  
142 values < 0.05 (\*) according to Tukey's multiple comparison and Dunn's method.

## 143 **Results**

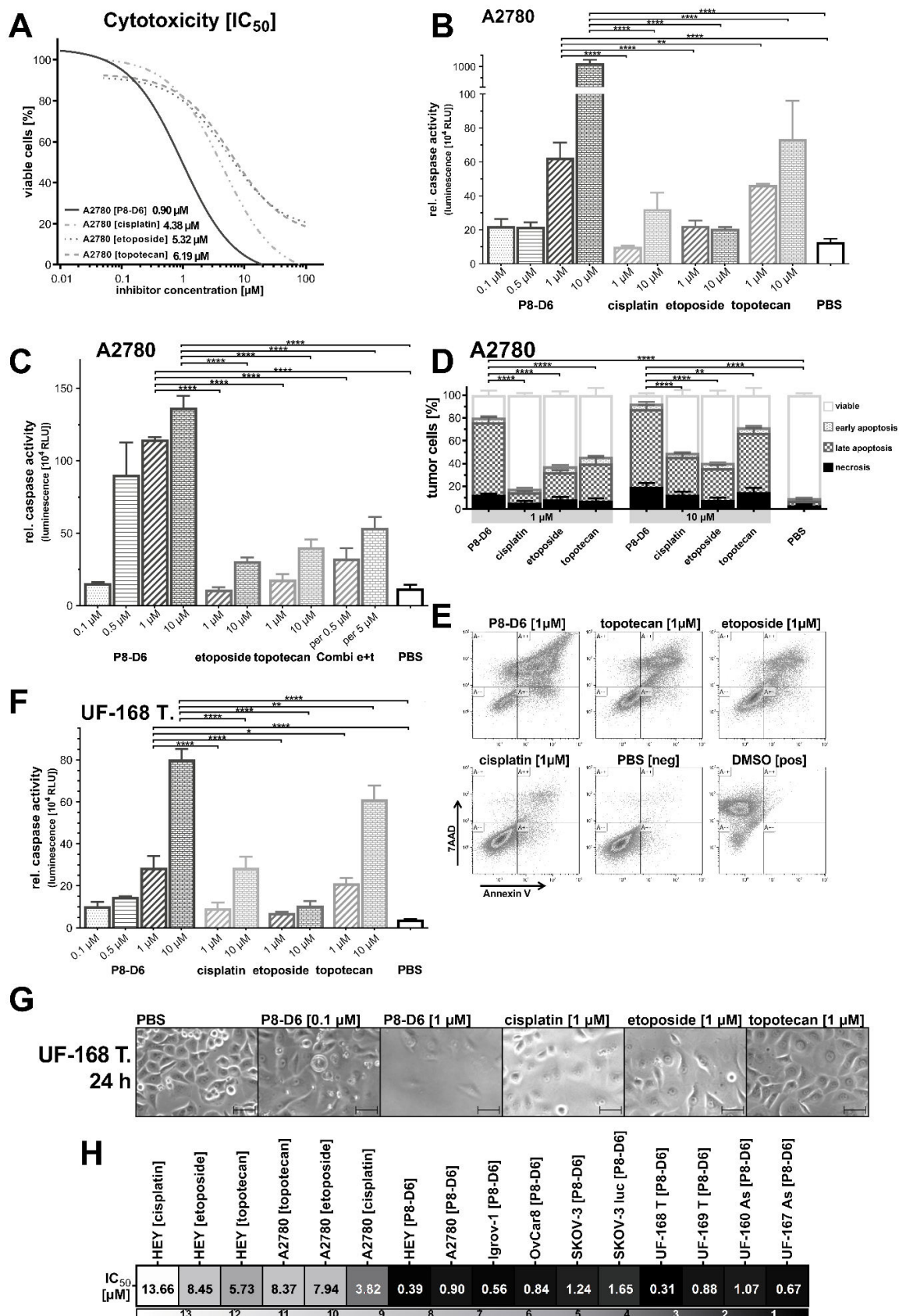
144 Previous studies showed that P8-D6 functions as dual topoisomerase inhibitor (4, 7). However,  
145 the effectiveness is highly dependent on reaching its nuclear target structure -topoisomerase I/II. In

146 addition to colon cancer cells (4), we checked the location of P8-D6 and Topo I and II expression in  
147 OvCa. Using fluorescent microscopy, P8-D6 was identified in the nucleus (Additional file 1A-B).  
148 Additionally, western blot provided evidence that all cells also express sufficient Topo I and Topo II  
149 (Additional file 1C).

### 150 **P8-D6 is highly effective in OvCa 2D monolayers**

151 The main aim of this study was to prove efficacy of P8-D6 in OvCa. Therefore, OvCa cell lines  
152 (A2780, Igrov-1, HEY, OvCar8, SKOV-3, SKOV-3luc) were treated with P8-D6, and compared to  
153 topotecan, etoposide and cisplatin. Initially, the viability of OvCa cells after 48 h treatment was  
154 measured using an enzymatic assay and IC<sub>50</sub>-values were determined. P8-D6 exhibits a four times  
155 lower IC<sub>50</sub>-value and is, therefore, significantly more effective than the standard chemotherapeutics  
156 (Fig. 2A, 2H; Additional file 2A). A significantly higher increase of apoptosis after 48 h treatment  
157 with P8-D6 compared to its standard therapeutic drugs could be observed in all tested OvCa cell  
158 lines by using ApoLive-Glo™ Multiplex Assay (Fig. 2B, Additional file 2B-F) and flow cytometric  
159 analyses (Fig. 2D-E; Additional file 3B).

160 Since P8-D6 is a dual topoisomerase inhibitor, but the reference substances primarily inhibit  
161 one of the enzymes only, a combination of a Topo I (topotecan) and a Topo II (etoposide) inhibitor  
162 was analysed. Compared to this combination, P8-D6 shows a significantly higher rate of apoptosis  
163 (Fig. 2C; Additional file 3A). To validate the pronounced induction of apoptosis and anti-  
164 proliferative effect of P8-D6 in primary cells, we used *ex vivo* patient-derived cells from tumour  
165 tissue and ascites in a translational aspect. A significantly higher rate of anti-proliferative and  
166 apoptotic effect was observed in primary cells by P8-D6 compared to comparative substances (Fig.  
167 2F; 2G; Additional file 2G-H). Altogether, we generated results of a plurality of different cells  
168 (established and primary cells) to emphasize the durable and robust effect of P8-D6 (Fig. 2H).



169

170 Fig. 2. Antitumour responses in OvCa 2D monolayers. A2780 (cell line) and UF-168T. (primary cells)

171 were treated with different concentrations of P8-D6, topotecan, etoposide, cisplatin and negative control

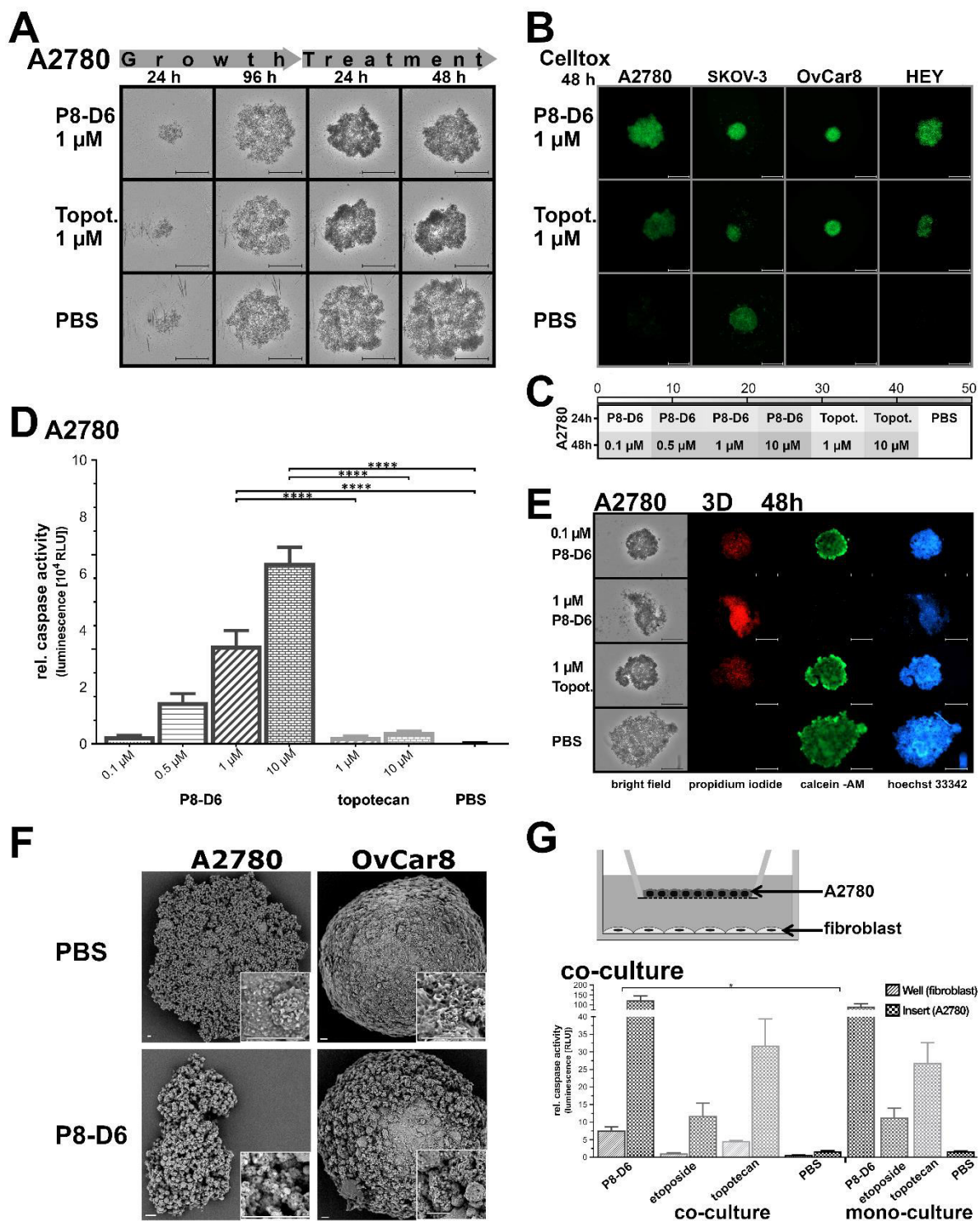
172 [PBS] for 48 h. Subsequently, the viability and caspase activity were determined. (A) The IC<sub>50</sub> values of  
173 each cytostatic drug were calculated by using the viability data. (B) The apoptosis is represented as  
174 relative caspase activity. (C) To compare the combinatorial apoptotic effect of topotecan (Topo I Inhibitor)  
175 and etoposide (Topo II Inhibitor) to P8-D6, a dual topoisomerase inhibitor was performed in A2780. (D)  
176 (E) Flow cytometric analysis of pro-apoptotic effects with Annexin V-PE (An V) and 7AAD staining (n=6).  
177 Representative flow cytometry dot plots of treated and stained A2780 cells were done. The mean  
178 distribution of viable (An V/7AAD-negative), early apoptotic (An V-positive, 7AAD-negative), late  
179 apoptotic/necrotic (An V/7AAD-positive) or necrotic (An V-negative, 7AAD-positive) tumour cells after  
180 treatment were calculated (D). (F) For primary OvCa cells (UF-168T.) viability and apoptosis were  
181 measured. (G) Additionally, the anti-proliferative effect after 24 h treatment was evaluated by microscopy.  
182 Scale bars, 50 µm. (H) Heat map of the IC<sub>50</sub> values using the viability of all tested OvCa cells. Data are  
183 means + SD one-way ANOVA, \* (p < 0.05), \*\* (p < 0.01), \*\*\* (p < 0.001), \*\*\*\* (p < 0.001).

#### 184 **P8-D6 induce strong effects in 3D target tumour and co-culture model**

185 3D cell cultures are regarded to bridge the gap from 2D to *in vivo* models, since cell-cell  
186 interaction is considerable for the efficacy of a substance. 3D spheroids mimic the physiological  
187 behaviour of solid tumours more closely (10, 11). Spheroids were generated in Ultra-Low  
188 Attachment (ULA) plates for 96 h and subsequently treated with P8-D6 or topotecan. The OvCa  
189 spheroids (A2780, SKOV-3, HEY, OvCar8) showed a decrease in growth behaviour and stability  
190 after P8-D6 treatment (Fig. 3A; Additional file 4A-C). Cell toxicity was increased in all spheroids by  
191 P8-D6 compared to topotecan and PBS (Fig. 3B-C; Additional file 4D-F). Furthermore, P8-D6  
192 exerted a significantly increased proapoptotic effect in all spheroids compared to control (Fig. 3D;  
193 Additional file 5A-C). To visualize the potency of P8-D6 in spheroids, a triple live-dead staining  
194 consisting of calcein-AM, PI, and hoechst 33342 was used (Fig. 3E, Additional file 5D-F). The  
195 decreased staining of calcein-AM and the increase of cells stained with PI, proved the strong  
196 cytotoxic effect of P8-D6. Additionally, P8-D6 treated cells showed disintegration of the spheroid  
197 and a considerably higher number of dead cells than topotecan. 10-fold lower dose of P8-D6

198 showed similar results as 1  $\mu$ M topotecan. Moreover, SEM identified surface changes of the  
199 spheroids like loss of membrane integrity due to treatment (Fig. 3F, Additional file 4G).

200 Additionally, it was investigated whether fibroblast-A2780 co-culture could mediate changes  
201 in cancer cell responses to anti-cancer drugs by affecting cell-cell interaction (Fig. 3G). Co-culture  
202 promotes the apoptosis induction significantly for P8-D6 treated cancer cells compared to mono-  
203 culture, while the co-culture treated cancer cells with etoposide and topotecan only exhibited  
204 minimal activity differences.



205

206

207

208

209

210

211

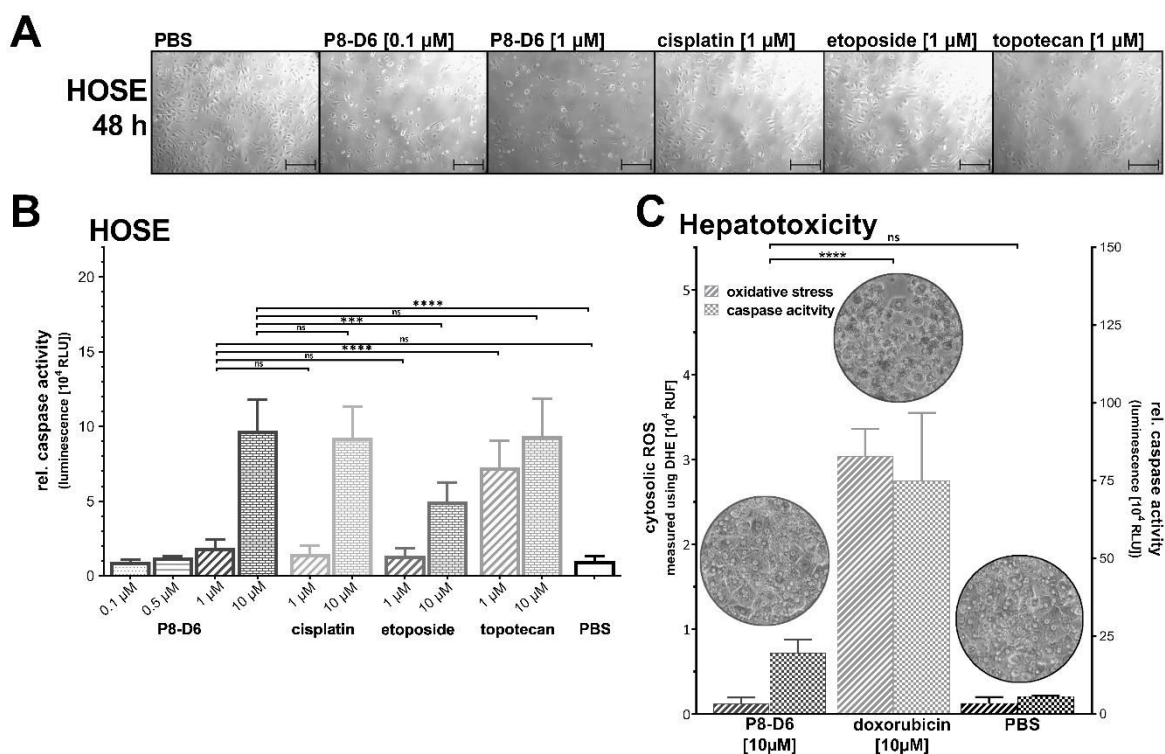
**Figure 3. Antitumour properties in 3D spheroids and 2D co-culture.** For 3D culture, A2780, SKOV-3, OvCar8 and HEY cells were maintained in ULA plates for 96 h and subsequently treated with P8-D6 [0.1  $\mu$ M, 0.5  $\mu$ M, 1  $\mu$ M, 10  $\mu$ M], topotecan [1  $\mu$ M, 10  $\mu$ M] and PBS for 48 h. (A) Every 24 h images were generated by microscopy. Scale bars, 500  $\mu$ m. (B) (C) During treatment the cell toxicity was measured by fluorescence microscope using CellTox™ Green (24 h, 48 h). Scale bars, 500  $\mu$ m. The fluorescence signals for 24 h and 48 h after treatment were quantified (fluorescence intensity RFU) and shown in a heat map

212 (C). (D) After 48 h treatment the viability and caspase activity were measured in A2780 spheroids. (E)  
213 A2780 spheroids were stained after the growth and treatment phase with PI (red), calcein-AM (green),  
214 hoechst 33342 (blue) and measured by microscopy. Scale bars, 500  $\mu\text{m}$ . (F) SEM images of A2780 and  
215 OvCar8 spheroids, which were treated with P8-D6 [1  $\mu\text{M}$ ] or PBS for 48 h were taken. Scale bars, 20  $\mu\text{m}$ .  
216 (G) For co-culture experiments, A2780 cells were seeded in 2D monolayers on transwell inserts and  
217 fibroblasts on well bottoms. For comparison, mono-cultures were cultured and treated with P8-D6  
218 [10  $\mu\text{M}$ ], etoposide [10  $\mu\text{M}$ ], topotecan [10  $\mu\text{M}$ ] and PBS in the same way. The apoptosis represented as  
219 relative caspase activity was measured in A2780 and fibroblasts. Data are means + SD (n=3) one-way  
220 ANOVA, \* (p <0.05), \*\* (p <0.01), \*\*\* (p <0.001), \*\*\*\* (p <0.001).

### 221 **P8-D6 only slightly affects non-cancer cells**

222 Since side effects often occur as a result of tumour therapy it is important to determine the  
223 toxicity of P8-D6 in preclinical setting on non-cancerous cells such as human ovarian surface  
224 epithelium cells (HOSE). HOSE were treated for 48 h and the anti-proliferative effect of P8-D6 is  
225 only slightly increased compared to the reference (Fig. 4A). While 1  $\mu\text{M}$  P8-D6 is highly effective on  
226 cancer cells no significant increase of apoptosis was measured compared to PBS control in HOSE  
227 cells. The application of 10  $\mu\text{M}$  P8-D6 shows a similar value as positive controls (Fig. 4B).

228 Hepatotoxicity is a common and serious side effect in chemotherapy. By measuring oxidative  
229 stress and induction of apoptosis after 48 h treatment in primary human hepatocytes, P8-D6  
230 showed no significant difference compared to PBS, while doxorubicin induces significant cell  
231 damage effects (Figure 5C). P8-D6 proved to be cytotoxic against OvCa cells without inducing cell  
232 death in hepatocytes.



233

234 **Fig. 4. Effects on non-cancer cells.** (A) To examine toxic effects of therapy, human ovarian surface  
 235 epithelial cells (HOSE) were treated with P8-D6, cisplatin, etoposide, topotecan and PBS for 48 h. The anti-  
 236 proliferative effect after 48 h treatment was evaluated by microscopy. Scale bars, 100 μm. (B) The viability  
 237 and apoptosis were measured after 48 h treatment in HOSE cells. Data are means + SD (n=6) one-way  
 238 ANOVA, \* (p<0.05), \*\* (p<0.01), \*\*\* (p<0.001), \*\*\*\* (p<0.001). (C) To investigate the hepatotoxicity,  
 239 primary human hepatocytes were treated with P8-D6, doxorubicin and PBS for 48 h. Afterwards,  
 240 microscopy images were taken, and apoptosis and oxidative stress measurements were performed. Data  
 241 are means + SD (n=3) one-way ANOVA, \* (p<0.05), \*\* (p<0.01), \*\*\* (p<0.001), \*\*\*\* (p<0.001).

## 242 Discussion

243 Since OvCa is one of the world's deadliest gynaecological malignancies, there is a high clinical need  
 244 for the development of new, effective and well-tolerated therapy options with suitable  
 245 physiochemical properties (1). P8-D6 was investigated as a novel dual topoisomerase inhibitor in  
 246 OvCa cell line and *ex vivo* patient derived primary cells in 2D, 3D and co-culture and was proven to  
 247 be overall significantly more effective than standard therapeutics and negative control.

248 Side effects due to chemotherapy have significant impacts on therapy. However, P8-D6 shows only  
249 limited toxic effects on normal cells. If efficacy and toxicity studies are related to clinical therapy,  
250 P8-D6 induces significantly higher (>five-fold) apoptosis rates in OvCa than current standards.  
251 Thus, it could potentially be used in lower doses than the standard therapeutic agents to achieve  
252 the same effect.

253 Due to the dual topoisomerase inhibition of P8-D6, the question arises whether a combination  
254 therapy of two established mono-Topo I/II inhibitors reach the antitumour potency of P8-D6 in  
255 OvCa. Previous studies compared the combination of Topo I with Topo II inhibitor versus  
256 monotherapy and showed heterogeneous results (18–21). This study showed significantly higher  
257 induction of apoptosis by P8-D6 when compared to the additive effect of Topo I and Topo II  
258 inhibitor combination. So far, the combination of topotecan and etoposide shows no clinical benefit  
259 (22) and is not considered as a clinical standard, whereas mono-therapy is (23).

260 A major advantage of a dual topoisomerase inhibitor is the reduced development of resistance  
261 through inhibition of both topoisomerases. The inhibition of only one enzyme causes a  
262 compensatory upregulation of the other (21, 24). The effectiveness of dual topo-inhibitors on solid  
263 tumours has been shown previously (25, 26). In clinical trials, however, these drugs showed  
264 intolerable side effects. (e.g. intoplicine, TA-103, batracylin), such as hepatotoxicity and severe  
265 neutropenia (26–32). Because of this increased hepatotoxicity with dual topoisomerase inhibitors  
266 (33), the hepatotoxicity of P8-D6 was determined. Importantly, this study shows that P8-D6 has no  
267 relevant effect concerning oxidative stress and apoptosis in human hepatocytes. The mechanism of  
268 action is the key benefit and novel about these drugs by affecting both topoisomerases. However, it  
269 is a validated target since single Topo inhibitors are already standards in cancer therapy (23).

270 The current therapy for platinum-resistant/refractory OvCa consists mainly of a monotherapy with  
271 topotecan or PLD, but cancer control rate is limited (34–36). Hence, some novel drugs are in clinical  
272 trials like the tyrosine kinase inhibitor rivoceranib (37). The antibody drug conjugate (ADC)  
273 Mirvetuximab soravtansine (MIRV) comprise a FR $\alpha$ -binding antibody, cleavable linker, and the

274 tubulin-targeting toxin DM4. A Phase III study evaluated the safety and efficacy of MIRV compared  
275 to chemotherapy in patients with platinum-resistant OvCa (38).  
276 A combination of P8-D6 with a tyrosyl-DNA phosphodiesterase inhibitor or a PARP inhibitor could  
277 merit additional consideration. These enzymes are involved in the repair mechanisms of the Topo-  
278 DNA complex and would possibly have a further positive effect in apoptosis induction (39, 40).  
279 Liposomal formulations could also be possible further approaches for P8-D6.

## 280 **Conclusions:**

281 In summary, P8-D6 has promising antitumour properties in 2D, 3D and co-culture in OvCa. It has  
282 fewer effects on normal ovarian cells and hepatocytes than its references. To sum up, P8-D6 is a  
283 strong and rapid inductor of apoptosis and warrants further development. Further *in vivo*  
284 experiments for P8-D6 are needed to verify antitumour effects also for complex multiorgan systems.  
285 Additionally, further studies on other side effects that could lead to dose-limitation should be  
286 performed.

## 287 **List of abbreviations**

288 2D, two-dimensional; 3D, three-dimensional; 5-FU, fluorouracil; ADC, antibody drug conjugate; DAPI, 4',6-  
289 Diamidin-2-phenylindol; FR $\alpha$ , Folate receptor alpha; GI50, Growth inhibitory of 50 %; HOSE, human ovarian  
290 surface epithelial cells; IC50, inhibitory concentration 50 %; MIRV, Mirvetuximab soravtansine; NCI, National  
291 Cancer Institute; OvCa, OvCa; PARP, Poly (ADP-ribose) polymerase; PI, propidium iodide; PLD, pegylated  
292 liposomal doxorubicin; RFU, relative fluorescence units; RLU, relative luminescence units; SD, standard  
293 deviation; SEM, scanning electron microscopy; Topo, topoisomerase; UKSH, university Hospital Schleswig-  
294 Holstein; ULA, Ultra-Low Attachment

## 295 **Declarations**

296 **Ethics approval and consent to participate:** Institutional Review Board Statement: The study was conducted  
297 according to the guidelines of the Declaration of Helsinki, and approved by the Institutional Review Board of  
298 the University Medical Centre Schleswig-Holstein, Campus Kiel (AZ: D578/20) and the Uppsala Regional  
299 Ethical Review Board (Ethical Approval no. 2009/028). Informed consent was obtained from all subjects  
300 involved in the study.

301 **Consent for publication:** Not applicable

302 **Availability of data and materials:** Not applicable

303 **Competing interests:** The authors declare that they have no competing interests.

304 **Funding:** This research received no external funding

305 **Author Contributions:** Conceptualization, I.F. and D.B.; investigation, I.F.; methodology, I.F., N.H., M.Ö.;  
306 resources, T.N.S. and B.C.; supervision, I.F., B.C. and D.B.; writing—original draft preparation, I.F.; writing—  
307 review and editing, T.N.S., N.H., M.Ö., P.A., B.C. and D.B. All authors have read and agreed to the published  
308 version of the manuscript.

309 **Acknowledgments:** We thank Dr. Marie Hellfritsch for assistance with SEM imaging. Sigrid Hamann and  
310 Catharina Verkooyen we thank for technical assistance.

311

312 Received \_\_\_\_\_ ; revised \_\_\_\_\_ ; accepted \_\_\_\_\_ ; published Online \_\_\_\_\_

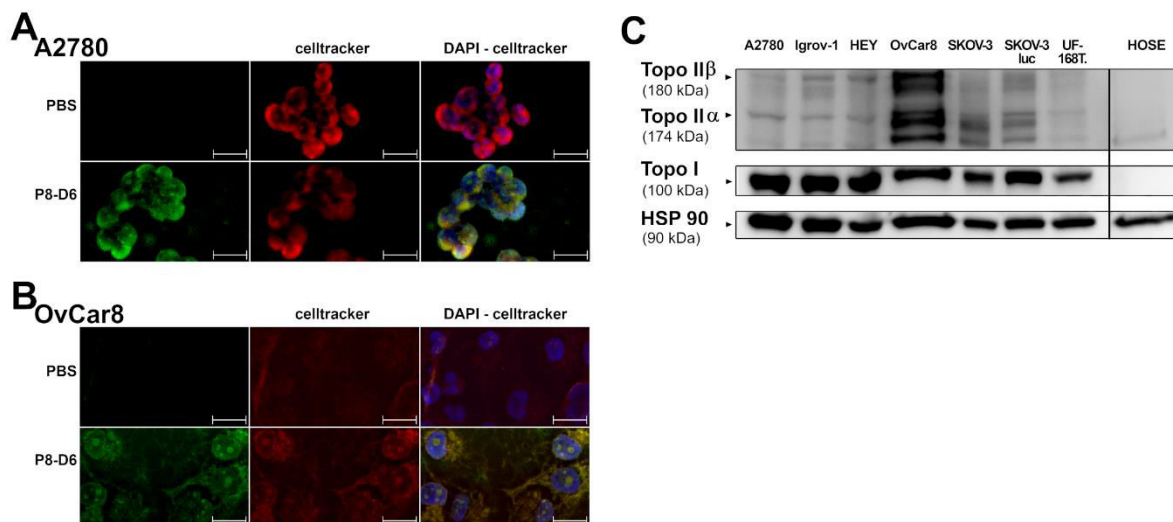
313

## 314 **References**

- 315 [1] Siegel RL, Miller KD, Jemal A. Cancer statistics, 2020. *CA Cancer J Clin* 2020;70(1):7–30.  
316 <https://doi.org/10.3322/caac.21590>.
- 317 [2] Ledermann JA. First-line treatment of ovarian cancer: Questions and controversies to address. *Ther Adv*  
318 *Med Oncol* 2018;10(15):1–8. <https://doi.org/10.1177/1758835918768232>.
- 319 [3] Chandra A, Pius C, Nabeel M, Nair M, Vishwanatha JK, Ahmad S et al. Ovarian cancer: Current status  
320 and strategies for improving therapeutic outcomes. *Cancer Med* 2019;8(16):7018–31.  
321 <https://doi.org/10.1002/cam4.2560>.
- 322 [4] Aichinger G, Lichtenberger F-B, Steinhauer TN, Flörkemeier I, Del Favero G, Clement B et al. The Aza-  
323 Analogous Benzo[c]phenanthridine P8-D6 Acts as a Dual Topoisomerase I and II Poison, thus Exhibiting  
324 Potent Genotoxic Properties. *Molecules* 2020;25(7):1524. <https://doi.org/10.3390/molecules25071524>.
- 325 [5] Pommier Y, Barcelo JM, Rao VA, Sordet O, Jobson AG, Thibaut L et al. Repair of topoisomerase I-  
326 mediated DNA damage. *Prog Nucleic Acid Res Mol Biol* 2006;81(1):179–229.  
327 [https://doi.org/10.1016/S0079-6603\(06\)81005-6](https://doi.org/10.1016/S0079-6603(06)81005-6).
- 328 [6] Deweese JE, Osheroff N. The DNA cleavage reaction of topoisomerase II: Wolf in sheep's clothing.  
329 *Nucleic Acids Res* 2009;37(3):738–48. <https://doi.org/10.1093/nar/gkn937>.
- 330 [7] Meier C, Steinhauer TN, Koczian F, Plitzko B, Jarolim K, Girreser U et al. A Dual Topoisomerase  
331 Inhibitor of Intense Pro-Apoptotic and Antileukemic Nature for Cancer Treatment. *ChemMedChem*  
332 2017;12(5):347–52. <https://doi.org/10.1002/cmdc.201700026>.
- 333 [8] National Cancer Institute. DTP homepage: Cancer Screen 09/2014: NCI-60 DTP Human Tumor Cell Line  
334 Screen. The National Cancer Institute (NCI) is gratefully acknowledged for its excellent screening service;  
335 Available from: <http://dtp.nci.nih.gov>.
- 336 [9] Edmondson R, Broglie JJ, Adcock AF, Yang L. Three-dimensional cell culture systems and their  
337 applications in drug discovery and cell-based biosensors. *Assay Drug Dev Technol* 2014;12(4):207–18.  
338 <https://doi.org/10.1089/adt.2014.573>.
- 339 [10] Goodman TT, Olive PL, Pun SH. Increased nanoparticle penetration in collagenase-treated multicellular  
340 spheroids. *Int J Nanomedicine* 2007;2(2):265–74.
- 341 [11] Kimlin LC, Casagrande G, Virador VM. In vitro three-dimensional (3D) models in cancer research: An  
342 update. *Mol Carcinog* 2013;52(3):167–82. <https://doi.org/10.1002/mc.21844>.
- 343 [12] Lagies S, Schlimpert M, Neumann S, Wäldin A, Kammerer B, Borner C et al. Cells grown in three-  
344 dimensional spheroids mirror in vivo metabolic response of epithelial cells. *Commun Biol* 2020;3(1):1–10.  
345 <https://doi.org/10.1038/s42003-020-0973-6>.

- 346 [13] Kurbacher CM, Korn C, Dixel S, Schween U, Kurbacher JA, Reichelt R et al. Isolation and Culture of  
347 Ovarian Cancer Cells and Cell Lines. *Methods Mol Biol* 2011(731):161–80. [https://doi.org/10.1007/978-1-61779-080-5\\_15](https://doi.org/10.1007/978-1-61779-080-5_15).
- 349 [14] Hedemann N, Herz A, Schiepanski JH, Dittrich J, Sebens S, Dempfle A et al. ADAM17 Inhibition  
350 Increases the Impact of Cisplatin Treatment in Ovarian Cancer Spheroids. *Cancers* 2021;13(9).  
351 <https://doi.org/10.3390/cancers13092039>.
- 352 [15] Ölander M, Wiśniewski JR, Flörkemeier I, Handin N, Urdzik J, Artursson P. A simple approach for  
353 restoration of differentiation and function in cryopreserved human hepatocytes. *Arch Toxicol*  
354 2018;93(3):819–829. <https://doi.org/10.1007/s00204-018-2375-9>.
- 355 [16] Huang X, Weimer J, von Wurmb-Schwark N, Fredrik R, Arnold N, Schem C. Alteration of STR profiles in  
356 ovarian carcinoma cells during primary culture. *Arch Gynecol Obstet* 2016;294(2):369–76.  
357 <https://doi.org/10.1007/s00404-016-4018-9>.
- 358 [17] Plitzko B, Havemeyer A, Kunze T, Clement B. The pivotal role of the mitochondrial amidoxime reducing  
359 component 2 in protecting human cells against apoptotic effects of the base analog N6-  
360 hydroxylaminopurine. *J Biol Chem* 2015;290(16):10126–35. <https://doi.org/10.1074/jbc.M115.640052>.
- 361 [18] Kaufmann SH. Antagonism between Camptothecin and Topoisomerase II-directed Chemotherapeutic  
362 Agents in a Human Leukemia Cell Line. *Cancer Res* 1991;51(4):1129–36.
- 363 [19] Bertrand R, O'Connor PM, Kerrigan D, Pommier Y. Sequential administration of camptothecin and  
364 etoposide circumvents the antagonistic cytotoxicity of simultaneous drug administration in slowly  
365 growing human colon carcinoma HT-29 cells. *Eur J Cancer* 1992;28(4-5):743–8.  
366 [https://doi.org/10.1016/0959-8049\(92\)90107-d](https://doi.org/10.1016/0959-8049(92)90107-d).
- 367 [20] Camacho KM, Kumar S, Menegatti S, Vogus DR, Anselmo AC, Mitragotri S. Synergistic antitumor  
368 activity of camptothecin-doxorubicin combinations and their conjugates with hyaluronic acid. *J Control*  
369 *Release* 2015;210(28):198–207. <https://doi.org/10.1016/j.jconrel.2015.04.031>.
- 370 [21] van Gijn R, Lendfers RRH, Schellens JHM, Bult A, Beijnen JH. Dual topoisomerase I/II inhibitors. *J Oncol*  
371 *Pharm Pract* 2000;6(3):92–108. <https://doi.org/10.1177/10781552000600303>.
- 372 [22] Sehouli J, Sommer H, Klare P, Stauch M, Zeimet A, Paulenz A et al. A randomized multicenter phase III  
373 trial of topotecan monotherapy versus topotecan + etoposide versus topotecan + gemcitabine for second-  
374 line treatment of recurrent ovarian cancer. *J Clin Oncol* 2006;24(18):5030.  
375 [https://doi.org/10.1200/jco.2006.24.18\\_suppl.5030](https://doi.org/10.1200/jco.2006.24.18_suppl.5030).
- 376 [23] Bookman MA, Brady MF, McGuire WP, Harper PG, Alberts DS, Friedlander M et al. Evaluation of new  
377 platinum-based treatment regimens in advanced-stage ovarian cancer: A Phase III Trial of the  
378 Gynecologic Cancer Intergroup. *J Clin Oncol* 2009;27(9):1419–25.  
379 <https://doi.org/10.1200/JCO.2008.19.1684>.
- 380 [24] Aronson JK (ed.). *Side Effects of Drugs Annual 27: Cytostatic drugs*. 1st ed. Amsterdam: Elsevier Science;  
381 2004.
- 382 [25] Skok Ž, Zidar N, Kikelj D, Ilaš J. Dual Inhibitors of Human DNA Topoisomerase II and Other Cancer-  
383 Related Targets. *J Med Chem* 2020;63(3):884–904. <https://doi.org/10.1021/acs.jmedchem.9b00726>.
- 384 [26] Denny WA, Baguley BC. Dual topoisomerase I/II inhibitors in cancer therapy. *Curr Top Med Chem*  
385 2003;3(3):339–53. <https://doi.org/10.2174/1568026033452555>.
- 386 [27] van Gijn R, Bokkel Huinink WW ten, Rodenhuis S, Vermorken JB, van Tellingen O, Rosing H et al.  
387 Topoisomerase I/II inhibitor intoplicine administered as a 24 h infusion: Phase I and pharmacologic  
388 study. *Anti-cancer Drugs* 1999;10(1):17–23. <https://doi.org/10.1097/00001813-199901000-00003>.
- 389 [28] Abigerges D, Armand JP, Chabot GG, Bruno R, Bissery MC, Bayssas M et al. Phase I and pharmacology  
390 study of intoplicine (RP 60475; NSC 645008), novel topoisomerase I and II inhibitor, in cancer patients.  
391 *Anticancer Drugs* 1996;7(2):166–74. <https://doi.org/10.1097/00001813-199602000-00004>.
- 392 [29] Ewesuedo RB, Iyer L, Das S, Koenig A, Mani S, Vogelzang NJ et al. Phase I clinical and pharmacogenetic  
393 study of weekly TAS-103 in patients with advanced cancer. *J Clin Oncol* 2001;19(7):2084–90.  
394 <https://doi.org/10.1200/JCO.2001.19.7.2084>.

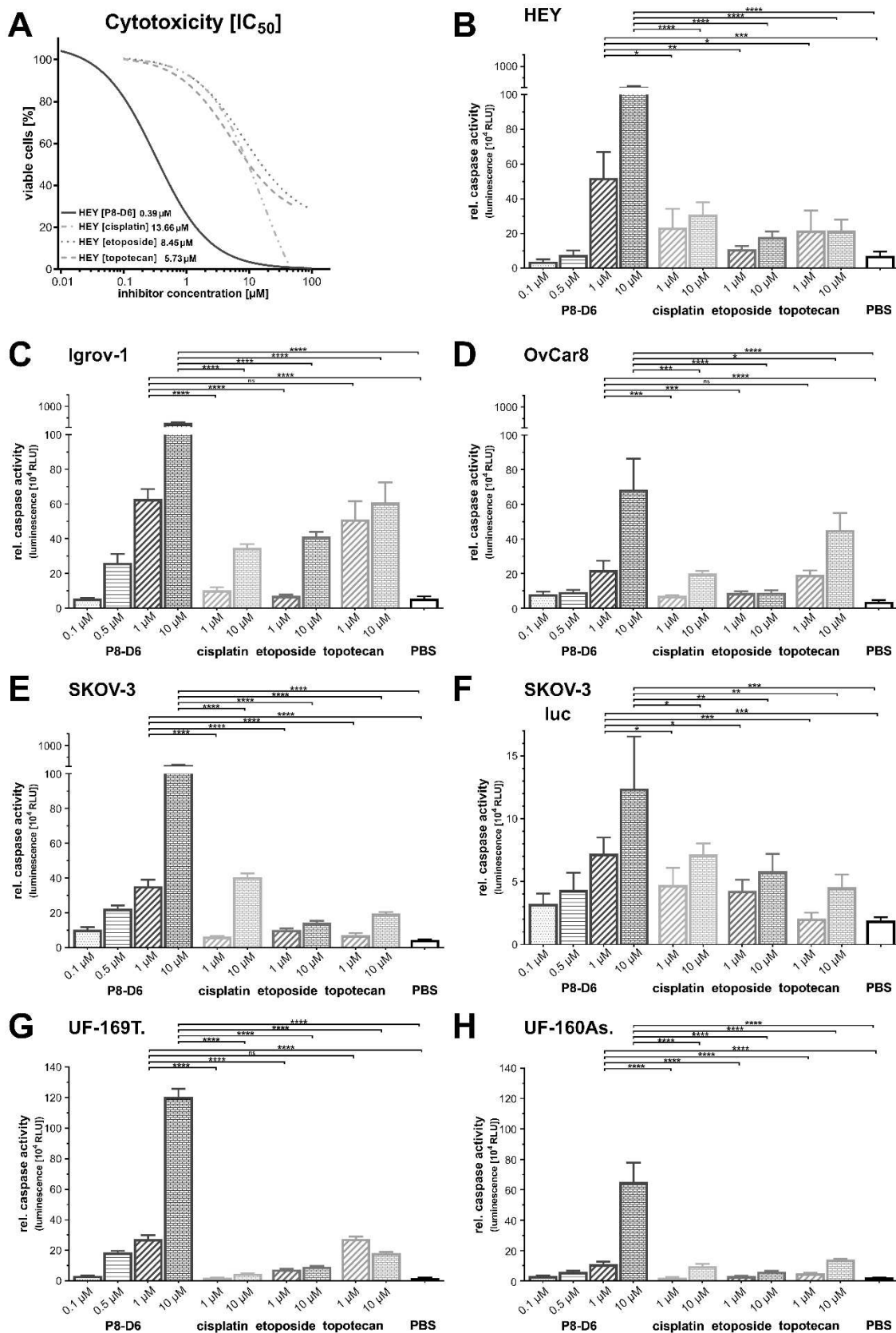
- 395 [30] Salerno S, Da Settimo F, Taliani S, Simorini F, La Motta C, Fornaciari G et al. Recent advances in the  
396 development of dual topoisomerase I and II inhibitors as anticancer drugs. *Curr Med Chem*  
397 2010;17(35):4270–90. <https://doi.org/10.2174/092986710793361252>.
- 398 [31] Kummur S, Gutierrez ME, Anderson LW, Klecker RW, Chen A, Murgu AJ et al. Pharmacogenetically  
399 driven patient selection for a first-in-human phase I trial of batracylin in patients with advanced solid  
400 tumors and lymphomas. *Cancer Chemother Pharmacol* 2013;72(4):917–23. [https://doi.org/10.1007/s00280-](https://doi.org/10.1007/s00280-013-2244-4)  
401 013-2244-4.
- 402 [32] Mucci-LoRusso P, Polin L, Bissery MC, Valeriote F, Plowman J, Luk GD et al. Activity of batracylin  
403 (NSC-320846) against solid tumors of mice. *Invest New Drugs* 1989;7(4):295–306.  
404 <https://doi.org/10.1007/BF00173759>.
- 405 [33] King PD, Perry MC. Hepatotoxicity of chemotherapy. *Oncologist* 2001;6(2):162–76.  
406 <https://doi.org/10.1634/theoncologist.6-2-162>.
- 407 [34] Rowinsky EK, Grochow LB, Hendricks CB, Ettinger DS, Forastiere AA, La Hurowitz et al. Phase I and  
408 pharmacologic study of topotecan: A novel topoisomerase I inhibitor. *J Clin Oncol* 1992;10(4):647–56.  
409 <https://doi.org/10.1200/JCO.1992.10.4.647>.
- 410 [35] Abushahin F, Singh DK, Lurain JR, Grendys EC, Rademaker AW, Schink JC. Weekly topotecan for  
411 recurrent platinum resistant ovarian cancer. *Gynecol Oncol* 2008;108(1):53–7.  
412 <https://doi.org/10.1016/j.ygyno.2007.08.062>.
- 413 [36] Ding D, Kong W-m. Analysis of relative factors of bone marrow suppression after chemotherapy with  
414 carboplatin and paclitaxel on the patients with ovarian cancer. *Zhonghua Fu Chan Ke Za Zhi*  
415 2011;46(3):188–92.
- 416 [37] Miao M, Deng G, Luo S, Zhou J, Le Chen, Yang J et al. A phase II study of apatinib in patients with  
417 recurrent epithelial ovarian cancer. *Gynecol Oncol* 2018;148(2):286–90.  
418 <https://doi.org/10.1016/j.ygyno.2017.12.013>.
- 419 [38] Moore K, Oza A, Colombo N, Oaknin A, Scambia G, Lorusso D et al. FORWARD I (GOG 3011): A phase  
420 III study of mirvetuximab soravtansine, a folate receptor alpha (FR $\alpha$ )-targeting antibody-drug conjugate  
421 (ADC), versus chemotherapy in patients (pts) with platinum-resistant ovarian cancer (PROC). *Annals of*  
422 *Oncology* 2019;5(30):403. <https://doi.org/10.1093/annonc/mdz250>.
- 423 [39] Murai J, Pommier Y. PARP Trapping Beyond Homologous Recombination and Platinum Sensitivity in  
424 Cancers. *Annu Rev Cancer Biol* 2019;3(1):131–50. [https://doi.org/10.1146/annurev-cancerbio-030518-](https://doi.org/10.1146/annurev-cancerbio-030518-055914)  
425 055914.
- 426 [40] Hall SR, Goralski KB. ZATT, TDP2, and SUMO2: Breaking the tie that binds TOP2 to DNA. *Translational*  
427 *Cancer Research* 2018;7(4):439–444. <https://doi.org/10.21037/tcr.2018.02.03>.
- 428

429 **Appendices**

430

431 **Additional file 1: Target control.** (A) (B) A2780 (A) and OvCar8 (B) were treated with 10  $\mu$ M P8-D6  
 432 (fluorophore: 462<sub>Ex</sub>/530<sub>Em</sub>) or negative control (PBS) for 30 min. Then cells were fixed, and membrane and  
 433 nucleus were stained by CellTracker™ Deep Red Dye and DAPI. Fluorescence images show the  
 434 fluorophore (green) on the left, membrane staining (red) in the middle and finally the combination of drug  
 435 (green), membrane (red) and nucleus (blue) staining on the right. Scale bars, 20  $\mu$ m. (C) Investigated cells  
 436 were lysed and protein expression was analysed by using western blot. All tested cells except for the non-  
 437 cancer HOSE cells are OvCa cells. HSP 90 was used as loading control.

438



439

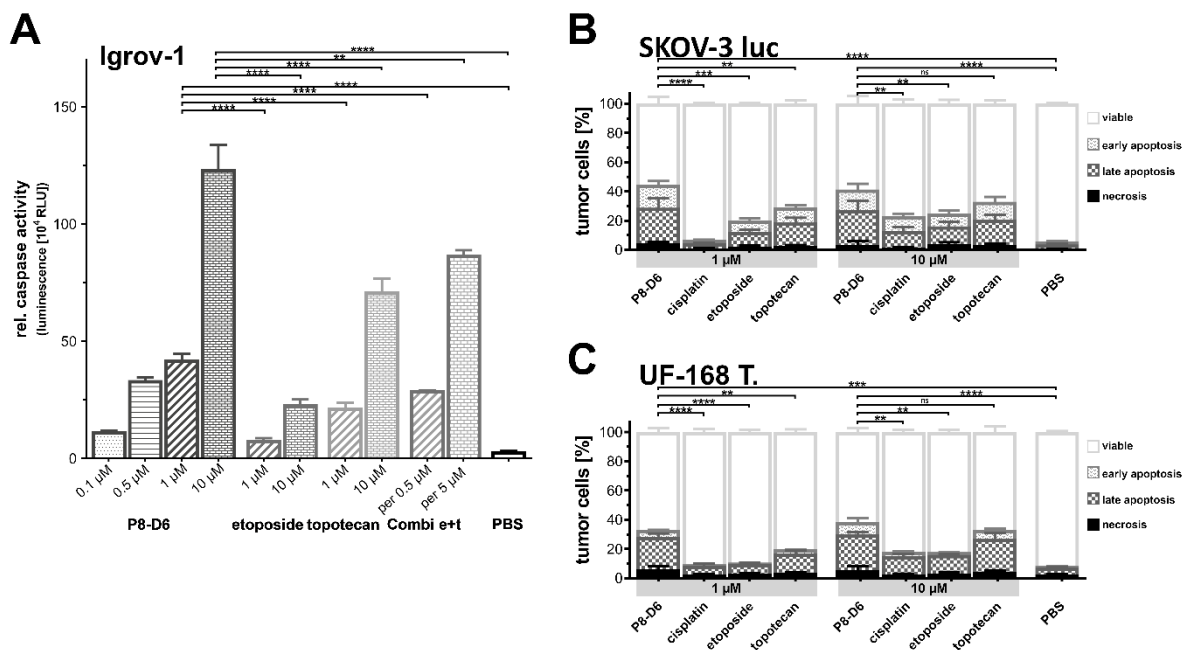
440

441

442

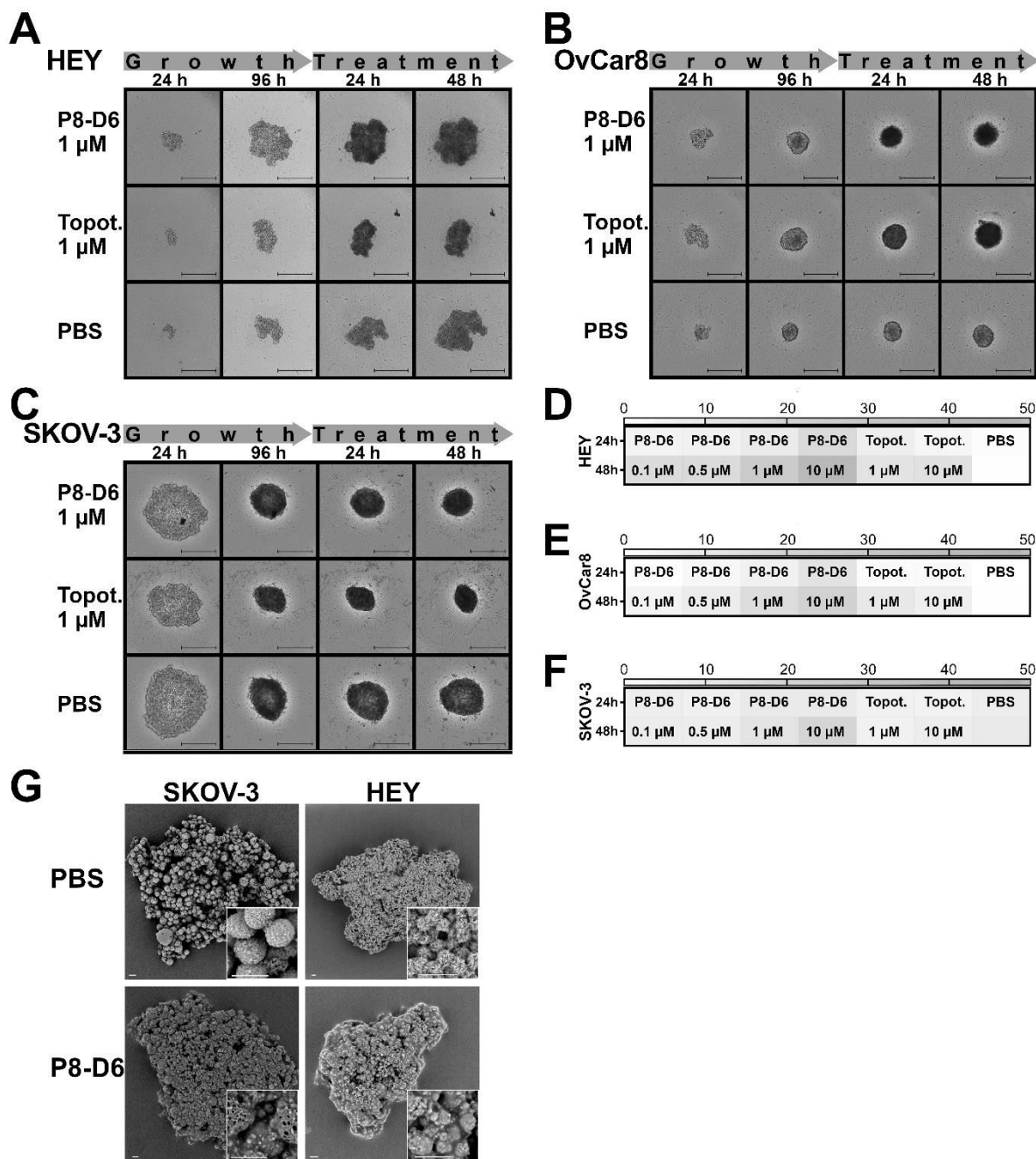
**Additional file 2: Cytotoxicity and apoptosis induction in OvCa 2D monolayers.** Ovarian cancer cells were treated with different concentrations of P8-D6, topotecan, etoposide, cisplatin and negative control [PBS] for 48 h. Afterwards the viability and caspase activity were determined. A) The IC<sub>50</sub> value of each

443 cytostatic drug in HEY cells was calculated by using the viability data. (B-H) The apoptosis is represented  
 444 as relative caspase activity in HEY (B), Igrov-1 (C), OvCar8 (D), SKOV-3 (E), SKOV-3luc (F) and primary  
 445 ovarian cancer cells UF-169T (G), UF-160AS (H), Data are means + SD one-way ANOVA, \* ( $p < 0.05$ ),  
 446 \*\* ( $p < 0.01$ ), \*\*\* ( $p < 0.001$ ), \*\*\*\* ( $p < 0.001$ )).



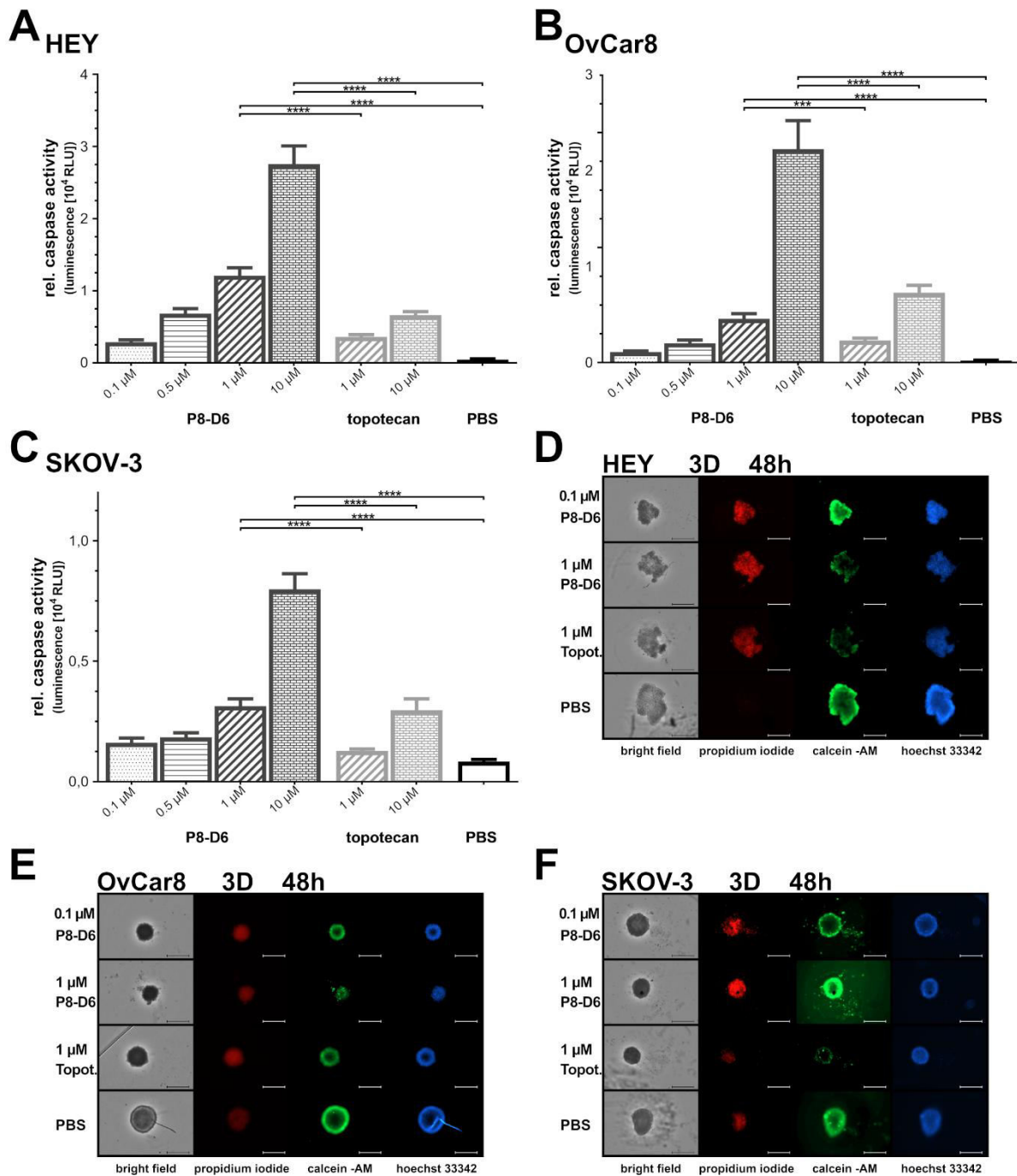
447

448 **Additional file 3: Apoptosis induction in OvCa 2D monolayers.** Ovarian cancer cells were treated with  
 449 different concentrations of P8-D6, topotecan, etoposide, cisplatin and negative control [PBS] for 48 h.  
 450 Afterwards, the apoptosis rate was determined. (A) Comparison of the combinatorial apoptotic effect of  
 451 topotecan (Topo I Inhibitor) and etoposide (Topo II Inhibitor) to P8-D6, a dual topoisomerase inhibitor  
 452 was performed in Igrov-1 after 48 h. (B) (C) Flow cytometric analysis of pro-apoptotic effects on SKOV-  
 453 3luc (B) and UF-168T. (C) cells after treatment and staining with Annexin V-PE and 7AAD ( $n=3$ ) were  
 454 done. The mean distribution of viable (An V/7AAD-negative), early apoptotic (An V-positive, 7AAD-  
 455 negative), late apoptotic/necrotic (An V/7AAD-positive) or necrotic (An V-negative, 7AAD-positive)  
 456 tumour cells after treatment were calculated (D). Data are means + SD one-way ANOVA, \* ( $p < 0.05$ ),  
 457 \*\* ( $p < 0.01$ ), \*\*\* ( $p < 0.001$ ), \*\*\*\* ( $p < 0.001$ )).



458

459 **Additional file 4: Morphological changes and cell toxicity in OvCa spheroids.** For 3D culture SKOV-3,  
 460 OvCar8 and HEY cells were maintained in ULA plates for 96 h and subsequently treated with P8-D6  
 461 [0.1  $\mu$ M, 0.5  $\mu$ M, 1  $\mu$ M, 10  $\mu$ M], topotecan [1  $\mu$ M, 10  $\mu$ M] and PBS for 48 h. (A-C) Every 24 h, images were  
 462 generated by microscopy (NYONE® Scientific (SYNENTEC)). Scale bars, 500  $\mu$ m. HEY (A), OvCar8 (B),  
 463 SKOV-3 (C). (D-F) During treatment, the cell toxicity was measured by fluorescence microscopy using  
 464 CellTox™ Green. The fluorescence intensities for 24 h and 48 h after treatment were quantified and shown  
 465 in heat maps. HEY (D), OvCar8 (E), SKOV-3 (F). (n=3) (G) SEM images of SKOV-3 and HEY spheroids,  
 466 which were treated with P8-D6 [1  $\mu$ M] or PBS for 48 h were taken. Scale bars, 20  $\mu$ m.



467

468

469

470

471

472

473

474

475

**Additional file 5: Apoptosis induction and live-dead staining in OvCa spheroids.** For 3D culture SKOV-3, OvCar8 and HEY cells were maintained in ULA plates for 96 h and subsequently treated with P8-D6 [0.1  $\mu$ M, 0.5  $\mu$ M, 1  $\mu$ M, 10  $\mu$ M], topotecan [1  $\mu$ M, 10  $\mu$ M] and PBS for 48 h. (A-C) After 48 h treatment, the viability and caspase activity were measured in HEY (A), OvCar8 (B) and SKOV-3 (C) spheroids. Data are means (n=3) + SD one-way ANOVA, \* (p < 0.05), \*\* (p < 0.01), \*\*\* (p < 0.001), \*\*\*\* (p < 0.0001). (D-F) HEY (D), OvCar8 (E) and SKOV-3 (F) spheroids were stained after growth and treatment phase with PI (red), calcein-AM (green), hoechst 33342 (blue) and measured by microscopy (NYONE® Scientific (SYNENTEC)). Scale bars, 500  $\mu$ m.